RETINAL FUNDUS IMAGE SEGMENTATION USING FUSIONNET

Deepak Anand, Mayank Kumar Singh and Amit Sethi

Department of Electrical Engineering, Indian Institute of Technology Bombay

ABSTRACT

Diabetic retinopathy (DR) is one of the most prevalent causes of avoidable vision impairment. The grading of DR requires a significant amount of time from an ophthalmologist. Indian Diabetic Retinopathy Image Dataset (IDRiD) challenge aimed at developing automated algorithms for the grading of DR and localization of lesions in the color fundus images. We have extensively used a previously proposed deep learning architecture known as FusionNet to tackle the tasks of optic disc segmentation and detection, exudate segmentation and combined segmentation of hemorrhages and microaneurysms. We achieved a Dice score of 0.74 for optical disc segmentation, 0.75 for hard exudate segmentation, and 0.58 for combined hemorrhages and microaneurysms. We also solved the optical disc detection subtask achieving an mean euclidean distance of 48.43 pixels.

Index Terms— IDRiD challenge, diabetic retinopathy, deep learning, FusionNet.

1. INTRODUCTION

Diabetic retinopathy (DR) is the most widespread cause of avoidable vision-impairment. According to World Health Organization (WHO), around 347 million people suffer from diabetes worldwide. Currently, detecting DR is a time-consuming process as well as the detectable symptoms often appear very late. DR grade is assessed based on the presence of different severity and extent of lesions and vascular abnormalities in the fundus images. The population of diabetic patients is on rise so there is a grave necessity for fast, accurate, and early detection of DR. Long term and extensive vision loss can be prevented if retinal lesions are detected early. However in developing countries such advances in treatments are often over-shadowed by the acute shortage of diagnosing physicians such as ophthalmologists. Computer-aided diagnosis can make mass-screening of retinal diseases possible.

There have been several attempts in past to develop algorithms for analyzing retinal fundus images for recognition of stage of DR using image-processing, pattern recognition and machine-learning. Analysis of DR has two subparts , first grading of DR and second segmentation of lesions. Several methods have been proposed for grading of DR [1, 2, 3]. Some of the most widely known methods were developed for a Kaggle competition on diabetic retinopathy [2]. The competition had goal of grading the color fundus images for DR. The grading of DR was to be done on the scale of 0-4 (0 - No DR, 1 - Mild, 2 - Moderate, 3 - Severe, and 4 - Proliferative DR). Figure 1 shows a representative image for non-proliferative and proliferated diabetic retinopathy. Some of the most successful methods have been, unsurprisingly, based on deep learning convolutional neural networks (CNNs). In [3], a CNN was trained to achieve state of the art classification results for two datasets EyePACS and Messidor-2.

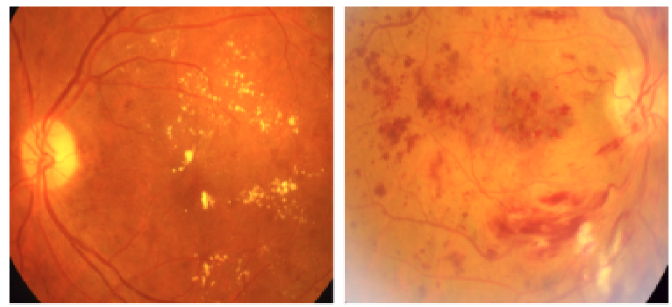

Fig. 1. Representative image for non-proliferative diabetic retinopathy (left) and proliferative diabetic retinopathy (right). Source: IDRiD Challenge Website.

There is a direct correspondence between the abnormality of growth of retinal blood vessels and severity of DR [4]. Thus many attempts have been made to segment blood-vessels in fundus images [4, 5, 6, 7]. Although retinal blood-vessel segmentation is a very well explored task by conventional image-processing [8], deep-learning has significantly improved upon the previous results, for example, [4] used an ensemble of convolutional neural networks (CNN) for retinal blood vessels segmentation on Digital Retinal Images for Vessel Extraction (DRIVE) dataset.

The Indian Diabetic Retinopathy image Dataset (IDRiD) challenge goes further than the Kaggle challenge and DRIVE dataset with the challenge to segment and identify different parts of the retina and types of lesions – optical disc, fovea, microaneurysms, memorrhages, hard exudates, and soft exu-

Authors thank Nvidia GPU Grant scheme for the GPUs used for this work.

dates. We report results on segmentation of optical disc (OD), hard exudates (EX), microaneurysms (MA), and hemorrhages (HA). We also address the detection of OD and fovea. Figure 3 shows examples of these regions in a representative image taken from the IDRiD dataset.

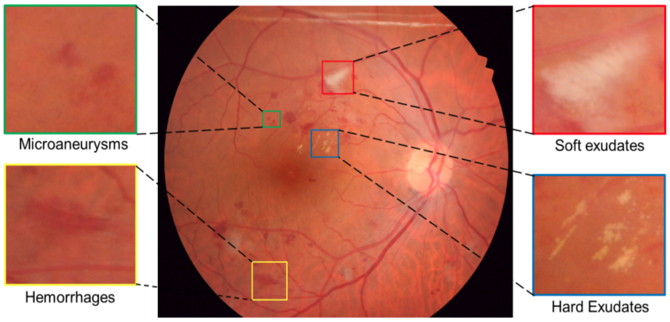

Fig. 2. Representative image for lesion segmentation. Source: IDRiD Challenge Website.

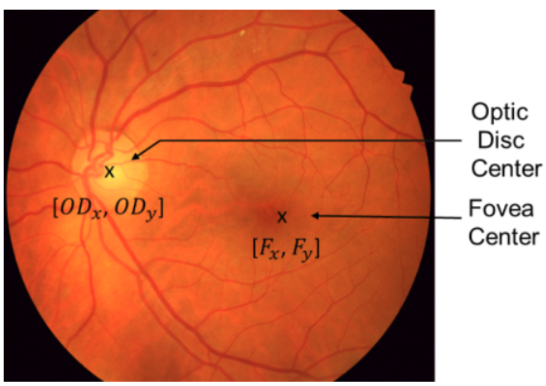

Fig. 3. Representative image showing Optical disc and Fovea. Source: IDRiD Challenge Website.

2. CNN ARCHITECTURE

We use the FusionNet architecture [9] throughout this paper for segmentation tasks. FusionNet is a fully convolutional network (FCN) which came as an improvement over the U-net architecture, [10]. It has a classical hour-glass structure of a U-net, and additionally, it has skip-connection and residual convolutional blocks. The architecture is shown in the Figure 4.

3. SUB-CHALLENGES

We now describe our processing steps and results for different sub-challenges in IDRiD challenge.

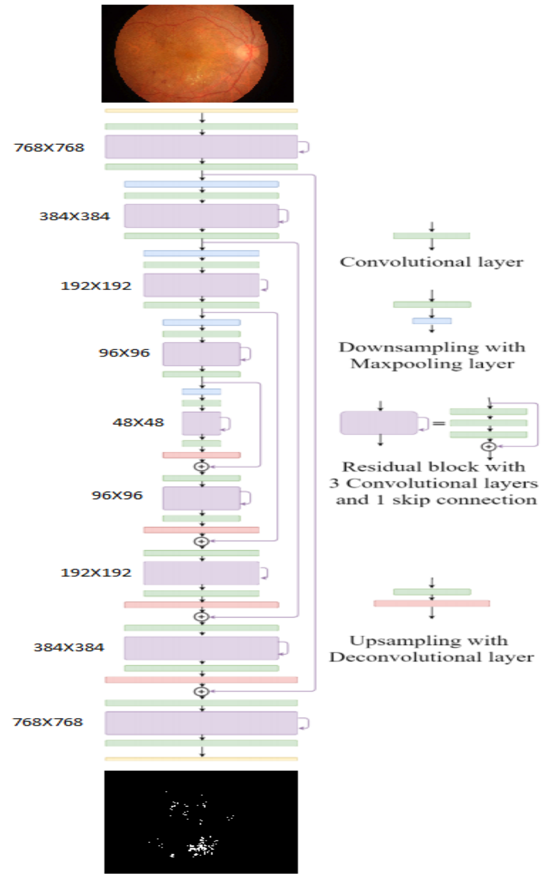

Fig. 4. Architecture of FusionNet used. Source : Original image from [9]

3.1. Optical Disc Segmentation and Detection

The segmentation of lesions in fundus images is often hindered by the bright intensity of optical disc. Therefore, we tackled the optical disc segmentation task first. The training dataset consists of 54 annotated images. Earlier works in segmentation of OD include hard-coded pre-processing of the images on the basis of intensity and thresholding [11, 12]. Due to the success of deep learning and FCNs for image segmentation, we decided to use deep learning, but the images were too big to fit on a single GPU. We have tackled this problem by first resizing the given images before feeding it into the FusionNet model. Due to some outliers (as in Figure 5), we had to post-process the results which increased the Dice score. The post-processing included finding contours in the predicted mask and taking that contour as the OD which was close to the center of the mass of the predicted mask. We do a 2-fold validation by splitting the training data and got a Dice-score of 0.7359.

To detect the central part of the optical disc we had a train-

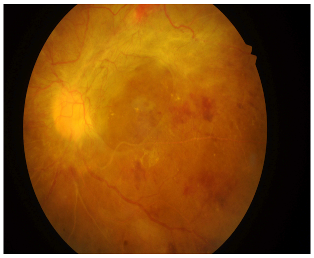

Fig. 5. Outlier image which contains high spreading of luminosity around the optical disc.

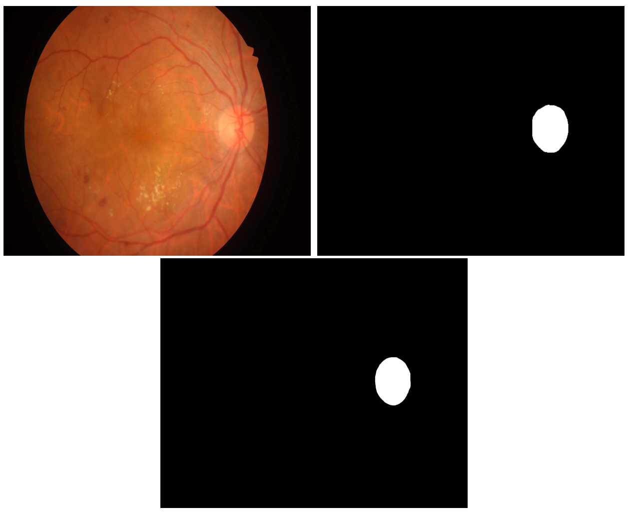

Fig. 6. OD segmentation results and annotations(Left to right, The original image, Our segmented Results) (bottom, The annotated image)

ing data of 413 images. The center of the optical disc was calculated as the centroid of the final segmented output of the optical disc segmentation. We achieve a mean euclidean distance of 48.43 pixels. An example of the results have been shown in Figure 6.

3.2. Hard exudate segmentation

Hard exudate are formed due to the accumulation of extracellular lipid from the retinal capillaries. It is quite common in diabetic macular edema due to leakage from damaged blood vessels. The segmentation dataset consisted of 54 annotated images. We deploy a FusionNet model for segmentation. We took patches of size 768$\times$768 for the segmentation of 512$\times$512 central area to take care of the edge effect and stitched it back to get the entire predicted image. The predicted and ground-truth images have been shown in Figure 7. We did a 2-fold validation by splitting the training data and got a Dice score of 0.7538.

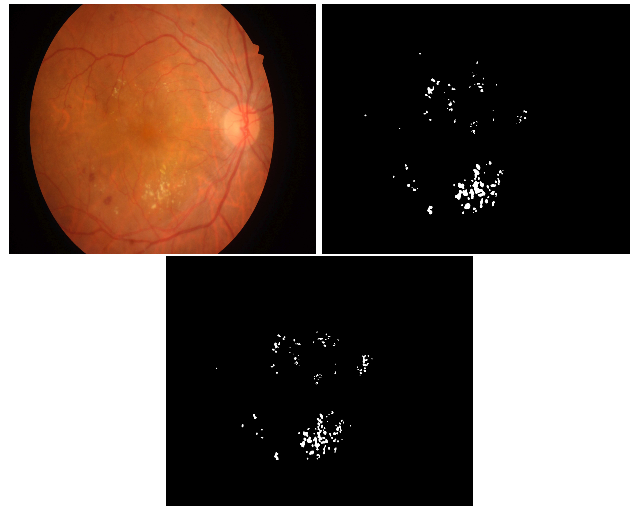

Fig. 7. Exudates segmentation results and annotations(Left to right, The original image, Our segmented Results) (bottom, The annotated image)

3.3. Microaneurysms and Hemorrhages segmentation

Microaneurysms are swelling of the retinal capillary and hemorrhages are its advanced form where blood leaks from ruptured capillary. We combined the task of segmenting hemorrhages (HE) and microaneurysms (MA), as distinguishing between hemorrhages and microaneurysms was challenging even for us. This can be attributed to the similar visual features of MA and HE because of blood color. Training dataset had 54 images. We have applied FusionNet for the combined segmentation task. The FusionNet is applied on the patch of size 768$\times$768, which gives the segmentation result for a central area of size 512$\times$512, to take care of the edge effect. The predicted patches of 512$\times$512 were stitched back together to get the predicted image. The results are as shown in 8. We performed a 2-fold validation by splitting the training data and got a Dice score of 0.5810.

4. CONCLUSION

We have used FusionNet for segmenting the optical disc, hemorrhages, microaneurysms and hard exudates. It seems to be a powerful framework for the challenge of detecting, recognizing, and segmenting various lesions in fundus images. Given multiple sub-challenges within the IDRiD challenge, we decided to leave segmentation of soft exudate and distinguishing between microaneurysms and hemorrhages as future work. Such fine-grained classification challenge can be built upon our segmentation results in the future. Though the images were large, due to JPEG compression too much data was lost, due to which the deep learning models could not make the full use of the large image size. Having high

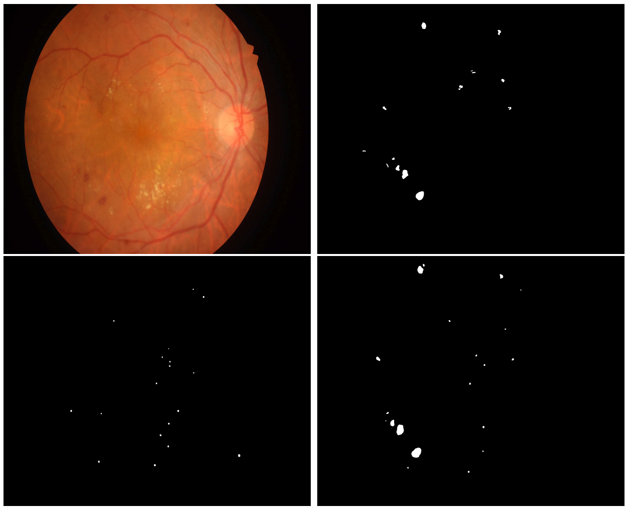

Fig. 8. MA and HE combined segmentation results (top left - The original image, top right - HE annotation, bottom left - MA annotation, bottom right - Combined predicted output)

quality images and annotations will further help improve the results making this usable in real-life applications.

5. REFERENCES

[1] Joon Yul Choi, Tae Keun Yoo, Jeong Gi Seo, Jiyong Kwak, Terry Taewoong Um, and Tyler Hyungtaek Rim, "Multi-categorical deep learning neural network to classify retinal images: A pilot study employing small database," *PloS one*, vol. 12, no. 11, pp. e0187336, 2017.

[2] California Healthcare Foundation and eyePACS, "Kaggle Competition: Diabetic Retinopathy Detection," .

[3] Varun Gulshan, Lily Peng, Marc Coram, Martin C Stumpe, Derek Wu, Arunachalam Narayanaswamy, Subhashini Venugopalan, Kasumi Widner, Tom Madams, Jorge Cuadros, et al., "Development and validation of a deep learning algorithm for detection of diabetic retinopathy in retinal fundus photographs," *Jama*, vol. 316, no. 22, pp. 2402–2410, 2016.

[4] Debapriya Maji, Anirban Santara, Pabitra Mitra, and Debdoot Sheet, "Ensemble of deep convolutional neural networks for learning to detect retinal vessels in fundus images," *arXiv preprint arXiv:1603.04833*, 2016.

[5] Zhun Fan, Jiewei Lu, Wenji Li, Caimin Wei, Han Huang, Xinye Cai, and Xinjian Chen, "A hierarchical image matting model for blood vessel segmentation in fundus images," *arXiv preprint arXiv:1701.00892*, 2017.

[6] Muhammad Moazam Fraz, Paolo Remagnino, Andreas Hoppe, Bunyarit Uyyanonvara, Alicja R Rudnicka, Christopher G Owen, and Sarah A Barman, "Blood vessel segmentation methodologies in retinal images–a survey," *Computer methods and programs in biomedicine*, vol. 108, no. 1, pp. 407–433, 2012.

[7] Gehad Hassan, Nashwa El-Bendary, Aboul Ella Hassanien, Ali Fahmy, Vaclav Snasel, et al., "Retinal blood vessel segmentation approach based on mathematical morphology," *Procedia Computer Science*, vol. 65, pp. 612–622, 2015.

[8] João VB Soares, Jorge JG Leandro, Roberto M Cesar, Herbert F Jelinek, and Michael J Cree, "Retinal vessel segmentation using the 2-d gabor wavelet and supervised classification," *IEEE Transactions on medical Imaging*, vol. 25, no. 9, pp. 1214–1222, 2006.

[9] Tran Minh Quan, David G. C. Hildebrand, and Won-Ki Jeong, "Fusionnet: A deep fully residual convolutional neural network for image segmentation in connectomics," *CoRR*, vol. abs/1612.05360, 2016.

[10] Olaf Ronneberger, Philipp Fischer, and Thomas Brox, "U-net: Convolutional networks for biomedical image segmentation," *CoRR*, vol. abs/1505.04597, 2015.

[11] G. B. Kande, P. V. Subbaiah, and T. S. Savithri, "Segmentation of exudates and optic disk in retinal images," in *2008 Sixth Indian Conference on Computer Vision, Graphics Image Processing*, Dec 2008, pp. 535–542.

[12] A. Basit and Muhammad Moazam Fraz, "Optic disc detection and boundary extraction in retinal images," *Appl. Opt.*, vol. 54, no. 11, pp. 3440–3447, Apr 2015.